Journal of Molecular and Cellular Cardiology 90 (2016) 120–128

Contents lists available at ScienceDirect

Journal of Molecular and Cellular Cardiology

journal homepage: www.elsevier.com/locate/yjmcc

Bone marrow transplantation modulates tissue macrophage phenotype and enhances cardiac recovery after subsequent acute myocardial infarction

Andrea Protti [a,b,1], Heloise Mongue-Din [a,1], Katie J. Mylonas [c], Alexander Sirker [a], Can Martin Sag [a,d], Megan M. Swim [c], Lars Maier [d], Greta Sawyer [a], Xuebin Dong [a], Rene Botnar [b], Jon Salisbury [e], Gillian A. Gray [c], Ajay M. Shah [a,*]

[a] Cardiovascular Division, King's College London British Heart Foundation Centre of Excellence, London, UK
[b] Division of Imaging Sciences and Bioengineering, King's College London British Heart Foundation Centre of Excellence, London, UK
[c] BHF/University Centre for Cardiovascular Science, University of Edinburgh, Queens Medical Research Institute, Edinburgh, UK
[d] Department of Cardiology, Universitätsklinikum Regensburg, Germany
[e] Department of Histopathology, King's College Hospital, London, UK

ARTICLE INFO

Article history:
Received 19 July 2015
Received in revised form 24 November 2015
Accepted 8 December 2015
Available online 11 December 2015

Keywords:
Bone marrow transplantation
Macrophage polarisation
Myocardial infarction

ABSTRACT

Background: Bone marrow transplantation (BMT) is commonly used in experimental studies to investigate the contribution of BM-derived circulating cells to different disease processes. During studies investigating the cardiac response to acute myocardial infarction (MI) induced by permanent coronary ligation in mice that had previously undergone BMT, we found that BMT itself affects the remodelling response.
Methods and results: Compared to matched naive mice, animals that had previously undergone BMT developed significantly less post-MI adverse remodelling, infarct thinning and contractile dysfunction as assessed by serial magnetic resonance imaging. Cardiac rupture in male mice was prevented. Histological analysis showed that the infarcts of mice that had undergone BMT had a significantly higher number of inflammatory cells, surviving cardiomyocytes and neovessels than control mice, as well as evidence of significant haemosiderin deposition. Flow cytometric and histological analyses demonstrated a higher number of alternatively activated (M2) macrophages in myocardium of the BMT group compared to control animals even before MI, and this increased further in the infarcts of the BMT mice after MI.
Conclusions: The process of BMT itself substantially alters tissue macrophage phenotype and the subsequent response to acute MI. An increase in alternatively activated macrophages in this setting appears to enhance cardiac recovery after MI.

1. Introduction

Bone marrow transplantation (BMT) is commonly used in experimental studies designed to investigate the specific contribution of BM-derived circulating cells to disease processes. The method involves irradiation of the recipient to ablate BM cells, followed by transplantation of donor BM, typically via intravenous infusion [1,2]. In mice after syngeneic BM transplantation, the BM, circulating and tissue pools of leukocytes are generally reconstituted within 2–3 weeks [1,2]. The use of BMT to generate chimeric mice with different gene expression in BM-derived cells versus host cells is a powerful approach in cardiovascular diseases [3–6].

Acute myocardial infarction (MI) evokes an initial inflammatory response involving infiltration by neutrophils, monocytes/macrophages and lymphocytes, during which the infarct undergoes repair and a fibrous scar is laid down. This is followed by a phase of infarct scar maturation, thinning and then gradual infarct expansion with adverse left ventricular (LV) remodelling. The latter results in ventricular dilatation and reduction in contractile function and involves significant changes in the non-infarcted myocardium, such as cardiomyocyte hypertrophy, interstitial fibrosis and other alterations in the extracellular matrix [7–9]. BMT in the context of acute myocardial infarction (MI) has been valuable in demonstrating the importance of macrophage-mediated inflammation [10,11] or the roles of BM-derived progenitor cells [12] in post-MI cardiac remodelling and dysfunction.

In the course of a study investigating responses to acute MI in mice that had undergone BMT, we found that the process of BMT itself substantially alters the response of the heart to acute MI. Here, we report

* Corresponding author at: Cardiovascular Division, James Black Centre, 125 Coldharbour Lane, London SE5 9NU, UK.
E-mail address: ajay.shah@kcl.ac.uk (A.M. Shah).
[1] Joint first authors.

http://dx.doi.org/10.1016/j.yjmcc.2015.12.007

that when acute MI is induced by permanent coronary ligation after BMT, there is a significantly enhanced cardiac contractile recovery and a reduction in adverse remodelling that is attributable to an altered tissue macrophage phenotype. This previously unrecognised effect may significant alter interpretation of studies involving BMT and MI and also provides new insights into the role of inflammatory cells in cardiac repair after MI.

2. Methods

Animal studies were conducted in accordance with the Guidance on the Operation of the Animals (Scientific Procedures) Act, 1986 (UK Home Office) and institutional guidelines. Studies were performed on C57BL/6 mice. The experimental protocol is shown in Supplementary Fig. 1.

2.1. BMT

BMT was performed using standard methods [13]. Mice aged 8–11 weeks were irradiated with a lethal dose of 9 Gy (9000 mSv). At 24 h, BM isolated from donor C57BL/6 mice was injected into the recipient via the tail vein at a dose of 9×10^7 cells in 200 μl. Briefly, donor BM was harvested in DMEM, filtered through a 40 μm cell strainer, washed in fresh DMEM, and then re-suspended in PBS at a final concentration of 4.5×10^8/ml. Animals were allowed to recover for 4 weeks. Female mice were used for most experiments. Survival was assessed in both male and female C57BL/6 mice.

2.2. Induction of MI

Permanent left coronary artery ligation was performed as described previously [14]. Animals were anaesthetised with 2% isoflurane/98% oxygen and ventilated via endotracheal intubation. A lateral thoracotomy was made in the fourth intercostal space. The pericardium was removed and the left coronary artery was ligated 1–2 mm below the tip of the left atrium. The chest wall was repaired in layers. Mice were allowed to recover in a warmed chamber for at least 6 h and treated with intramuscular buprenorphine and subcutaneous flunixin for perioperative analgaesia.

2.3. Cardiac magnetic resonance imaging (CMRI)

CMRI was performed at 3, 10 and 21 days after surgery on a 7T horizontal scanner (Agilent, Varian Inc., Palo Alto, CA). The gradient coil had an inner diameter of 12 cm, gradient strength of 1000 mT/m (100 G/cm) and rise-time of 120 μs. A quadrature transmit/receive coil (RAPID Biomedical GmbH, Germany) with an internal diameter of 39 mm was used. Anaesthesia was maintained with 1.5% isoflurane and a mix of O_2/medical air. Body temperature was maintained at 37° using a warm air fan. The ECG was monitored via two metallic electrodes placed subcutaneously in the front paws. A pressure-transducer for respiratory gating was placed on the abdomen. Simultaneous ECG triggering and respiration gating (SA Instruments) was applied.

The CMRI protocol included (a) T1-weighted acquisition of functional/volumetric and anatomical parameters [15]; (b) T1-weighted acquisition for late gadolinium enhancement (LGE) after intraperitoneal (i.p.) injection of 0.75 mmol/kg of gadolinium DPTA (Magnevist, Schering Healthcare, UK) [15]; and (c) T2*-weighted acquisition for haemosiderin localisation and T2* evaluation. LGE scans were performed 20–30 min post-injection on day 3 post-MI to evaluate the infarcted area. Heart rates ranged from 400 to 500 bpm (cycle length 120–150 ms) with a fluctuation of ±10 ms per cardiac cycle.

Cine-FLASH was used as a T1-weighted method for temporally resolved dynamic short-axis cardiac images to quantify functional/volumetric parameters and LGE acquisitions. Imaging parameters were: repetition time (TR) = 1 RR-interval/number of frames (typically ~9–10 ms), effective repetition time (TReff) = RR-interval, echo time (TE) = 1 ms, field of view (FOV) = 25 × 25 mm, matrix size = 128 × 128, slice thickness = 1 mm; flip angle = 40°, 3 averages, 9–11 slices, 1 k-space line/frame, 9–12 frames equally distributed along the cardiac cycle. The acquisition time was 8 ± 0.5 min. Triggering was positioned at the peak of the QRS complex. Single ECG gating was used to maintain a steady-state during acquisition in T1 weighted scans.

Cine-FLASH was also used as a T2*-weighted method to locate areas of signal void and the related T2* value. Imaging parameters were: TR = 3 RR-intervals (≈400 ms); TE = 1, 2, 3, 5, 7 ms; single frame acquired, typically the diastolic frame; FOV = 25 × 25 mm^2; matrix size = 128 × 128; slice thickness = 1 mm; number of slices = 5; flip angle = 40°; 3 averages; scanning time = 12 ± 0.5 min. ECG and respiration triggering were used, although, during respiration, signal acquisition and RF pulses were turned off. The trigger was positioned at the peak of the QRS complex corresponding to the diastolic phase.

T2* values were achieved by applying a T2* fit to the multi-echo T2*-weighted cine-FLASH images (TE varying from 1 to 7 ms) using ImageJ (NIH, Bethesda, MD). The T2* fitted followed the following equation:

$S = S0\ exp.(-TEn/T2^*)$.

where *S0* is the signal at full magnetisation, TE is the echo time and *n* identifies the echo time under study. Areas of rapid signal decay, affected by strong susceptibility effects, were compared to the control infarcted myocardium where a drop in signal was much less severe.

LV ejection fraction (EF), LV end-diastolic volume (LVEDV), LV end-systolic volume (LVESV) and LV mass were obtained from cine-FLASH T1-weighted images [16] using custom segmentation analysis software (www.clinicalvolumes.com). The initial infarct area (as a percentage of the LV) was analysed from cine-FLASH LGE images 3 days post-MI [15]. On subsequent scans, the extension of the infarct through the LV was quantified using a mid-line method [17]. The wall thickness along infarcted regions was evaluated by measuring the endocardium to epicardium distance using ImageJ software (NIH, Bethesda, MD) on the middle slice of CMRI images at 21 days post-MI.

2.4. Histology and immunostaining

Hearts were harvested and immediately immersed in 10% formalin for 48 h at 4 °C. Hearts were then embedded in paraffin and sectioned in 5 μm-thick transverse slices. After deparaffinisation and rehydration, sections were stained with haematoxylin-eosin (H&E), Prussian blue and Picrosirius red.

Cardiomyocytes were stained with an anti-troponin I antibody (Abcam, Cambridge, UK). The thickness of the infarct was evaluated in representative slices taken in the middle of the heart by measuring the endocardium to epicardium distance using ImageJ software (NIH, Bethesda, MD). Rhodamine-conjugated wheat germ agglutinin (WGA) was used to outline cell membranes. Large vessels and capillaries were labelled with anti-sm22α and isolectin B4 antibodies, respectively. Leukocytes were labelled using an anti-CD45 antibody (BD Biosciences, USA), detected with an HRP/DAB system followed by haematoxylin counterstaining. A similar procedure was used to detect CD163 (Bioss Inc., USA), a receptor involved in clearance and endocytosis of haemoglobin/haptoglobin complexes by macrophages [18], and VCAM-1.

Imaging was performed on an Olympus IX-81 microscope. Quantification was performed in a blinded fashion, using Volocity® software (PerkinElmer, USA).

2.5. Flow cytometry (FACS)

Quantitative analyses of LV macrophage number and phenotype were performed by FACS on tissue digests. Residual blood was first rinsed from the LV which was then dissected into infarcted and remote myocardium for separate analysis. Samples were digested in a mixture of collagenase IV, DNase and hyaluronidase at 37 °C for 30 min followed by trituration and filtration through a 70 μm nylon mesh. Cell suspensions were washed

and blocked with anti-CD16/CD32 antibodies prior to staining. Macrophages were identified as $CD45^+$, lineage negative ($CD19^-$, $CD3^-$, $NK1.1^-$, $Ly6G^-$), $CD11b^+F4/80^+$ cells and quantified for both Ly6C and MRC1 (CD206) expression. 7-amino-actinomycin D dye was used to identify dead cells (Supplementary Fig. 2).

FACS of leukocytes in male mice is described in Supplementary Materials. Fluorescence-minus-one (FMO) stained samples were used as negative controls. Experiments were performed on a FACS CantoII® instrument (BD Biosciences, New Jersey). Data analysis was performed with FlowJo software (Tree Star Inc., USA).

FACS was also performed on blood samples to study leukocyte and monocyte subsets (see Supplementary Materials).

2.6. Statistics

Data are reported as mean ± SEM. Comparisons of groups were undertaken by Student's *t* test or two-way ANOVA followed by Bonferroni's post-test, as appropriate, using GraphPad Prism 5.00. Kaplan–Meier survival analysis was performed over a 7-day period following MI. $P < 0.05$ was considered significant.

3. Results

3.1. Effect on BMT on infarct size and remodelling post-MI

Female mice that had undergone BMT and matched control animals ($n = 10$ per group) were subjected to left coronary ligation and then followed up for 21 days. We used serial CMRI to assess the initial infarct size, subsequent LV remodelling, contractile function and final infarct size. The two groups had similar LVESV, LVEDV and EF prior to MI (Fig. 1A–C). The initial infarct size estimated by LGE on CMRI 3 days post-MI was approximately 40% of the LV in both groups (Fig. 1E). In line with this, LVESV, LVEDV and EF were similar in the control and BMT groups at 3 days post-MI (Fig. 1A–C). By 7 and 21 days post-MI, there was a progressive increase in LVEDV and LVESV and a decrease in EF in the control MI group, indicating adverse LV remodelling. In contrast, the BMT MI group showed substantially lower increases in LVEDV and LVESV at these time-points while EF was significantly higher than in the control group (Fig. 1A–C). The relative infarct area as a percentage of the LV remained approximately 40% at 7 and 21 days in the control group (Fig. 1F). However, the relative infarct area gradually decreased at 7 and 21 days in the BMT group (Fig. 1F), indicating altered LV remodelling and/or scar properties. The wall thickness in the infarcted region on CMRI at 21 days was significantly higher in the BMT than control group (Fig. 1D). LV mass measured post-mortem (21 days post-MI) was significantly higher in the control group than the BMT group (113.5 ± 11.2 mg versus 74.3 ± 7.5 mg; $p < 0.05$). These results indicate that the BMT group had significantly less adverse remodelling post-MI than the control group despite a similar initial infarct size.

We analysed survival over a 12 day period after MI in a cohort of female control and BMT mice. This showed significantly higher survival in the mice that had undergone BMT (Fig. 1G). We performed a similar study in male C57BL/6 mice, which are known to have a higher rate of infarct rupture and mortality post-MI [19], and again found significantly higher survival in the BMT group (Fig. 1H).

3.2. CMRI evidence of T2* signal voids in the infarcted area after BMT

T2*-weighted CMRI at 21 days in the BMT group showed significant signal voids in the infarcted tissue in the absence of contrast injection, a

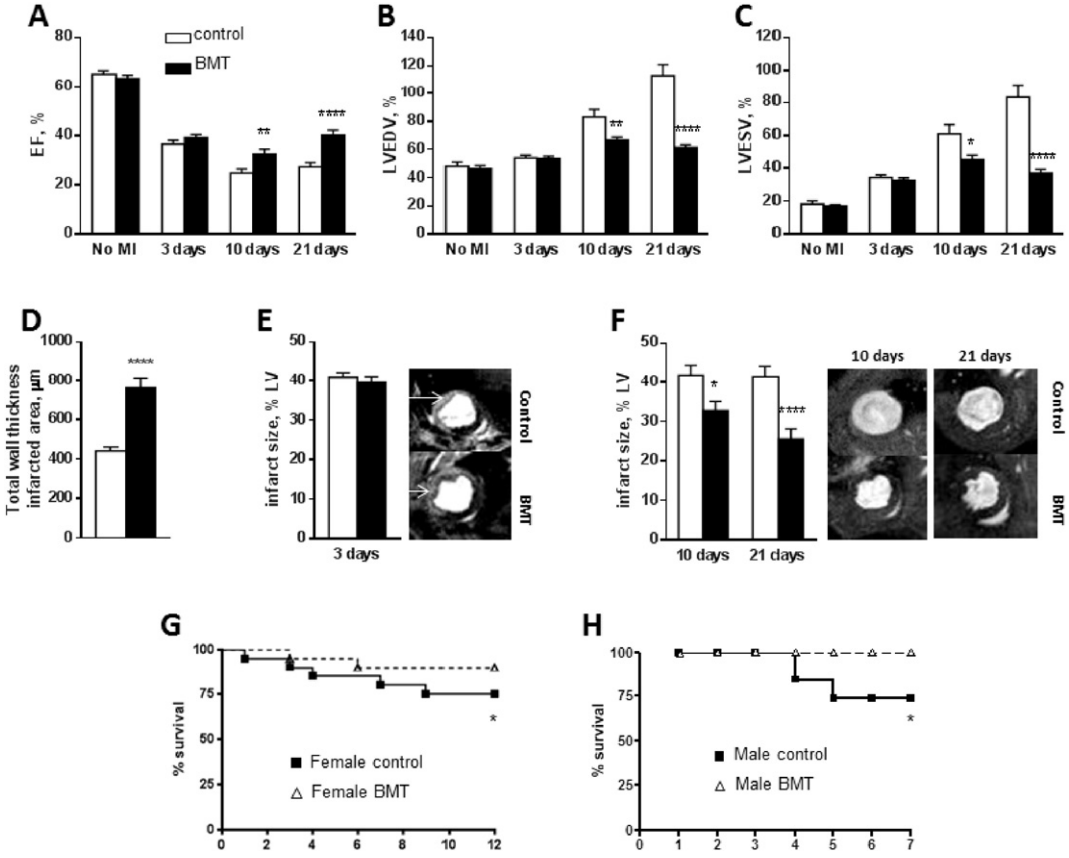

Fig. 1. Functional and volumetric cardiac parameters after MI in control and BMT mice. A–C: Ejection fraction (EF), left ventricle end diastolic volume (LVEDV) and left ventricle end systolic volume (LVESV) assessed by CMRI. D: Wall thickness in the infarct region. E: Infarct size 3 days post-MI, evaluated by late Gadolinium enhancement (LGE). Representative images are shown to the right. F: Infarct size at 10 and 21 days post-MI, calculated by a midline method. Representative images are shown to the right. G–H: Survival curves for female mice ($n = 20$/group) and male mice ($n = 21$ control, $n = 9$ BMT) subjected to MI. Bar graph data are mean ± SEM. *$p < 0.05$, **$p < 0.01$, ****$p < 0.0001$.

finding that was never observed in the control MI group. Fig. 2A shows representative apex-to-base short axis T2*-weighted images of control and BMT mice 21 days after MI. The signal void in the BMT heart, starting at the point of LAD ligature, continues in the following 2 slices towards the apex, indicating the presence of a susceptibility source in the infarcted tissue. Little or no signal void was detected in any of the groups at 3 and 10 days.

During T2* acquisitions, a susceptibility source is characterised by three main effects: (a) a negative signal area; (b) expansion of such an area with increasing TE; (c) T2* values much lower than the surrounding tissues. Fig. 2B demonstrates that when TE was increased from 1 to 7 ms, the signal void area significantly increased. The T2* values related to these signal voids were 2.37 ± 0.30 ms in the infarct area of the BMT group while remote areas and myocardium in the control group had a value of 13.45 ± 0.74 ms. In the absence of administration of iron-based contrast agents, signal voids of this type are most likely to be due to the presence of haemosiderin within the infarct, as a breakdown product of haemoglobin or myoglobin [20,21].

3.3. Histological findings

We undertook detailed histological comparison of the infarct region in control and BMT groups 21 days after induction of MI (Fig. 3). The LV wall at the infarcted site was thicker in the BMT compared to the control group on sections stained for troponin I. LV wall thickness in the infarcted area was greater in the BMT animals compared to controls (236 ± 22 μm vs. 327 ± 36 μm; $p < 0.01$; Fig. 3B). Though MRI and histology gave a similar trend, absolute values were different because of the post mortem processing of the sample.

At high power, there was a small endocardial rim of cardiomyocytes evident on H&E and troponin staining in the control group and only the very occasional cardiomyocyte within the scar (Fig. 4A, B). The scar tissue comprised predominantly fibroblasts (identified by their elongated nuclei) and collagen, with occasional areas of inflammatory cells but no vascular structures (Fig. 4C, D). The BMT infarct showed substantially more cardiomyocytes, present in the subendocardium, subepicardium and within the infarct itself. These myocytes were of similar size to those in the remote myocardium consistent with them being surviving myocytes. There were also significantly more inflammatory cells, most of them being macrophages, based on their morphology. CD45 immunostaining confirmed the higher level of mononuclear cell infiltration in the infarct area of the BMT group (Fig. 4E, F). Interestingly, most of the macrophages had a spindle-shaped dendritic morphology, a characteristic of alternatively activated (or M2) macrophages [22,23].

In view of the signal voids observed on CMRI, we performed Prussian blue-staining to look for iron (haemosiderin) deposition. The low magnification images revealed extensive iron deposition within the infarcted area in the BMT group whereas minimal staining was observed in the control group (Fig. 3A). At high magnification, the Prussian Blue staining was found to be predominantly intracellular within the spindle-shaped macrophages, which we consider is most likely related to the phagocytosis of dead haem-containing cells such as cardiomyocytes or erythrocytes and the breakdown of myoglobin or haemoglobin (Fig. 4G, H). Interestingly, CD163-positive macrophages (which have been implicated in the clearance of haemoglobin/haptoglobin complexes) were more abundant in the BMT than control group (Fig. 4I, J).

Infarcts in the BMT group also contained many irregular vascular structures typical of granulation tissue, which were not observed in the control infarcts (Fig. 4K–O). Positive staining for isolectin B4 and sm22α in the infarcts of the BMT group confirmed the presence of vessels and indicated that they mostly had a smooth muscle component.

The overall histological structure of the remote myocardium was similar in the control and BMT groups. However, the level of interstitial fibrosis was significantly higher in the control than the BMT group (Supplementary Fig. 3).

Taken together, these results indicate that LV wall in the infarct region in the BMT group is thicker than the control group, with more

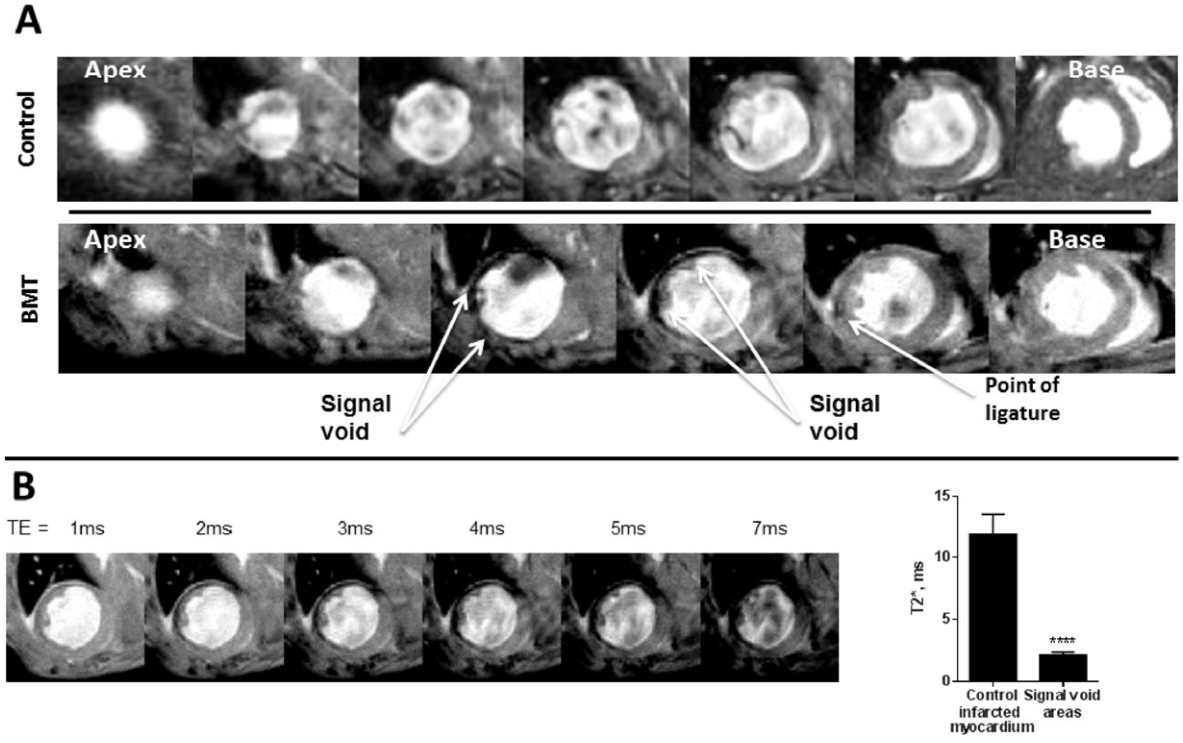

Fig. 2. Representative images of T2* signal voids observed on CMRI performed 21 days post-MI. A: Apex to base short axis CMR images for control and BMT mice 21 days post-MI. There are pronounced signal voids co-localised with the infarct region in the BMT mouse heart but no voids are seen in the control heart. B: T2* effects were studied by imaging the myocardium at multiple echo times (TE). The T2* of signal void areas was significantly lower than that of the control infarct region. Intramyocardial signal voids, caused by iron susceptibility effects, represent the presence of haem. Bar graph data are mean ± SEM. ***$p < 0.001$.

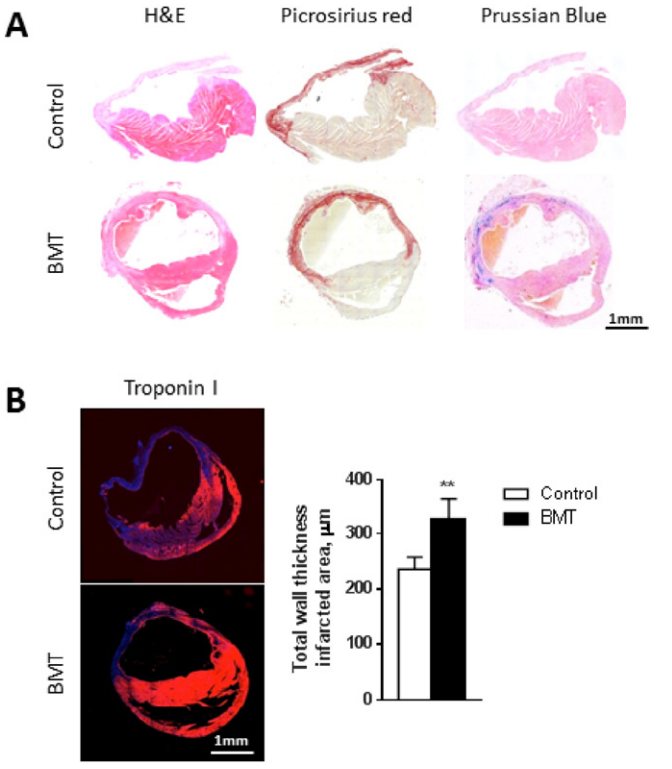

Fig. 3. Infarct thickness is increased in the BMT group. A: Representative transverse cross-sections of the whole heart from control and BMT mice 21 days post-MI. Sections are stained with haematoxylin and eosin (H&E), Picrosirius red and Prussian blue. The infarct region (bright red staining with Picrosirius red) is thicker and has robust Prussian blue staining in the BMT heart. B: Transverse cross-sections stained with an anti-troponin I antibody (red) for cardiomyocytes. The histogram shows the thickness of the LV in the infarcted region, measured at high magnification. Data are mean ± SEM from 5 hearts per group. $^{**}p < 0.01$.

surviving cardiomyocytes, more inflammatory cells (including many with haemosiderin within them) and frequent vascular structures.

3.4. BMT increases myocardial macrophage infiltration even before MI

To more carefully characterise and quantify the inflammatory cell infiltrate, we analysed the macrophage population in myocardial tissue digests by flow cytometry. In a sub-group of mice, using the CD45.1/CD45.2 chimaera system that exploits the different allelic forms of the pan-leukocyte marker CD45, we were able to distinguish between donor (CD45.1) and host-derived cells (CD45.2) after irradiation and BMT. This analysis showed that BMT results in replacement of >92% of the host cardiac macrophage population by donor cells and >93% blood monocytes (Supplementary Fig. 4). The overall number of neutrophils, monocytes, and T and B lymphocytes were similar in animals that had undergone BMT and controls (Supplementary Table 1).

Prior to MI, the total number of leukocytes ($CD45^+$) in the heart was 3-fold higher in the BMT group compared to control (Fig. 5A). The number of $CD11b^+/F4/80^+$ macrophages per mg of tissue was significantly higher in the BMT group and included both classically activated (M1) $Ly6c^{hi}$ cells and alternatively activated (M2) $MRC1^+$ cells (Fig. 5B–D). However, the proportion of alternatively activated macrophages (i.e. either $Ly6c^-$ cells or $MRC1^+$ cells) relative to total macrophages was substantially higher in the BMT than control group (Fig. 5E–H). This is supported by the observation in male mice that BMT hearts contain a significantly greater proportion of Mac2-immunoreactive macrophages (Supplementary Fig. 5A) and also of YM-1 positive M2-like macrophages (Supplementary Fig. 5B) than non-irradiated controls.

We next analysed circulating blood monocyte subsets in mice that had undergone BMT as compared to control mice. This revealed a significant increase in $Ly6c^-$ and $MRC1^+$ cells as a proportion of total monocytes in the BMT compared to control group (Supplementary Fig. 6). To assess whether the potential for polarisation into M1 versus M2-type macrophages is altered after BMT, we studied bone marrow-derived macrophages (BMDMs) from the BMT and control groups. Analysis of in vitro polarisation into M1 or M2 phenotypes revealed that there was no difference between the groups (Supplementary Fig. 7). We assessed if the myocardial vascular bed properties were altered by BMT Supplementary Fig. 8). There was no difference in capillary density between the BMT and control groups. However, myocardial vessels had enhanced endothelial VCAM-1 staining in the BMT group, suggestive of endothelial activation.

Taken together, these results indicate that BMT results in an increase in myocardial macrophages, especially alternatively activated macrophages, which may be related both to an increase in circulating $Ly6c^-/MRC1^+$ cells and to myocardial endothelial activation.

3.5. Increased myocardial macrophage infiltration after BMT and MI

Fig. 6 shows the characterisation of cells within the myocardium in the acute inflammatory phase 4 days post-MI. As expected, there was a substantial increase in total leukocytes and macrophages in the infarct region of both groups of animals (Fig. 6A, B). However, the extent of increase after MI was much higher in the BMT group, so that the cell number was 5–6 fold higher than the control group. Furthermore, there was a significant macrophage infiltration in the remote non-infarcted area in the BMT group. Overall numbers of $Ly6c^-$ and $MRC1^+$ cells were significantly greater in the BMT compared to control group, both in the infarcted and remote areas (Fig. 6C–F).

4. Discussion

The main finding of this study is that mice that have previously undergone BMT display a significantly altered structural and functional cardiac response to acute permanent coronary artery occlusion, with less thinning of the wall in the infarct region, reduced ventricular dilatation and better preserved contractile function than matched naive mice also subjected to acute MI. The enhanced recovery from acute MI in mice that have undergone BMT is associated with a significantly altered myocardial macrophage polarisation phenotype, comprising an increased number of alternatively activated (M2) macrophages in the myocardium.

Whilst undertaking a serial CMRI study to assess post-MI remodelling in mice that had undergone BMT, we noticed that the BMT group did not develop the same degree of LV dilatation and adverse remodelling as observed in control animals without BMT. The difference between groups became apparent from 1 to 3 weeks after MI whereas there were no significant differences in cardiac volumes and function early (3 days) after MI, consistent with a similar initial insult. Indeed, the initial infarct size estimated by LGE at 3 days post-MI was similar in the 2 groups. Serial CMRI showed that the LV wall in the infarct region did not thin to a similar extent in the BMT group as in control mice. Furthermore, animals that had undergone prior BMT showed higher survival after MI than control mice, both in females and in a model of more severe MI in male mice where there is a significant (around 25%) incidence of cardiac rupture.

Detailed histological analysis confirmed the presence of a thicker LV wall in the infarct region in the BMT group compared to the control group. It was notable that the infarcts in the BMT group had more layers of cardiomyocytes in the subendocardial and subepicardial regions than in control infarcts. Because the morphology and size of these cardiomyocytes was similar to that of myocytes in the remote non-infarcted regions, this finding may reflect a higher proportion of surviving cardiomyocytes in the BMT group. However, we did not undertake a

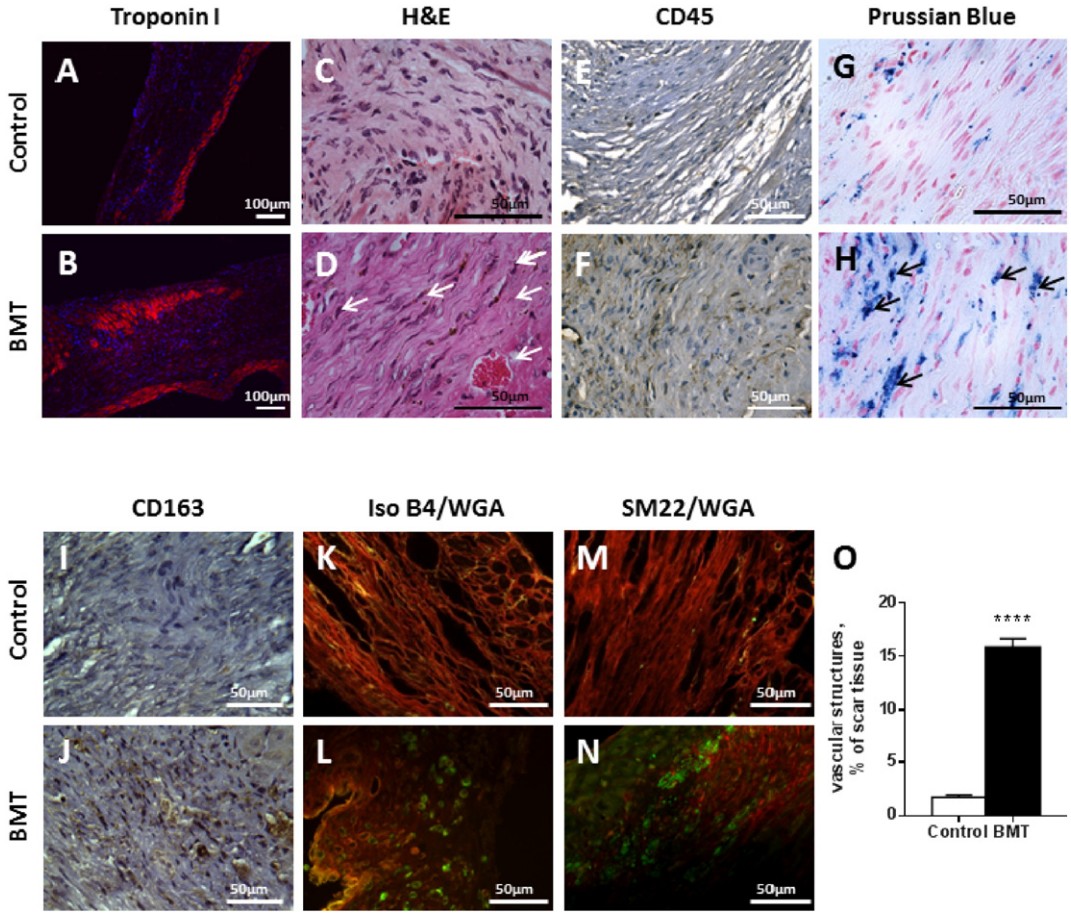

Fig. 4. Representative high magnification images showing increased inflammatory cells and neovessels in BMT compared to control infarcts. A, B: Troponin I staining (red) shows cardiomyocytes in both the epicardial and endocardial regions of the infarct in the BMT group whereas the control infarct only has a thin layer of subendocardial cardiomyocytes. Nuclei are stained with Dapi (blue). C, D: H&E staining reveals an accumulation of fibroblasts and mononuclear cells in the infarct. Arrows indicate spindle-shaped M2 macrophages. E, F: Immunostaining of CD45 positive cells (leukocytes, brown cytosolic staining) shows significantly more cells in the BMT group. G, H: Prussian blue staining shows intracellular hemosiderin (arrows) in the BMT group. I, J: Increased CD163-positive macrophages are observed in the BMT infarct. K–N: Irregular vascular structures are frequently observed in the BMT infarct, labelled for endothelial cells with Isolectin B4 (K, L — green) or for smooth muscle with anti-sm22α (M, N — green). Rhodamine-conjugated wheat germ agglutinin (WGA, red) was used to outline cell membranes. O: Quantification of the area within infarcts that was occupied by vascular structures. Sections stained for Isolectin B4 and WGA were observed at 40× magnification. Data are mean ± SEM from 3 random fields per infarct and 5 hearts per group. ****$p \leq 0.0001$.

detailed analysis of cardiomyocyte numbers in these hearts. The alternative possibility that there might have been cardiomyocyte regeneration within the infarct appears unlikely because this is reported to be associated with smaller cardiomyocytes over a 3 week post-MI period [24]. The overall fibrous tissue within the infarcts appeared similar in the BMT and control groups. The increased LV wall thickness in the infarct region of the BMT group, potentially related to an increased number of cardiomyocytes, is highly likely to be the explanation for the reduced degree of post-MI adverse remodelling, as a consequence of lower wall stress in the infarct region (regardless of whether these myocytes perform useful contractile work) [25].

Histological analysis also revealed that the infarcts of the BMT group contained substantially more inflammatory cells than control infarcts. We noted the presence of many irregular vascular structures in the infarcts of the BMT group. These neovessels usually had a smooth muscle coating, suggesting some degree of maturation. The pattern of inflammatory cell infiltration after acute MI in the mouse has been well documented [26]. It is well established that different subsets of monocytes/macrophages are present in the infarct; $Ly6c^{hi}$ cells are the predominant subtype during the first 1–2 days, after which time $Ly6c^{low}$ macrophages begin to predominate [26–28]. The $Ly6c^{hi}$ macrophages, also known as classically activated macrophages, typically produce pro-inflammatory cytokines, generate reactive oxygen species (ROS) and have a high scavenging activity. Conversely, the $Ly6c^{low}$ (alternatively activated or M2) macrophages secrete high levels of anti-inflammatory cytokines (e.g. interleukin-10), modulate the inflammatory response, are pro-angiogenic, and are thought participate in tissue repair [29]. Mannose receptor MRC1 (CD206) and Ym-1 expression also identifies the M2 subset [30–32]. Histologically, the macrophages in the infarcts of BMT mice were mostly spindle-shaped cells suggestive of M2 macrophages [22,23]. We therefore investigated the pattern of myocardial macrophage infiltration in the early phase of MI based on the expression of Ly6c and MRC1 [30,31,33]. Quantitative flow cytometric analysis of infarct and non-infarct regions revealed a substantially higher number of M2 macrophages ($Ly6c^{-}$ and $MRC1^{+}$) in the infarcts of the BMT group early after MI than in control mice, confirming the histological findings.

An additional striking observation at CMRI in the BMT/MI group was the presence of T2* intramyocardial signal voids, which is strongly suggestive of the presence of highly ferromagnetic haemosiderin (or ferritin). Histological analysis by Prussian blue staining confirmed the presence of substantially more iron in the infarcts of the BMT group and demonstrated that the staining was predominantly intracellular. Interestingly, the intracellular iron was sequestered predominantly in the spindle-shaped macrophages. The most likely sources of iron in the setting of MI are either from myoglobin from dead cardiomyocytes or from haemoglobin derived from extravasated blood. Although intra-infarct haemorrhage is more likely to occur in reperfused infarcts than with

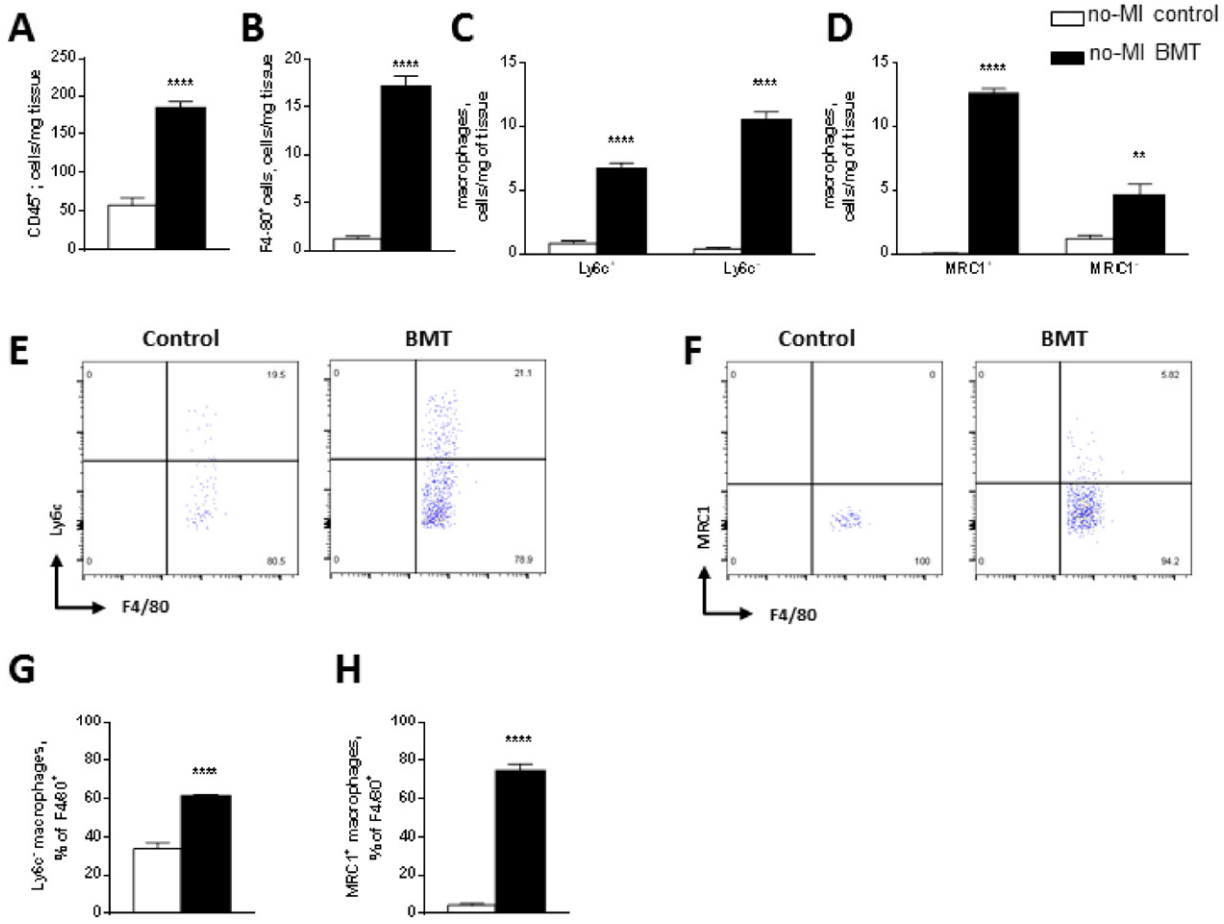

Fig. 5. BMT promotes infiltration of monocytes/macrophages into the myocardium even before MI. Flow cytometric analyses of inflammatory cells in LV myocardial digests of hearts from control and BMT mice before induction of MI. A–D: Quantification of total leukocytes (A), macrophages (B), and macrophage subsets according to expression of Ly6c (C) or MRC1 (D). E, F: Representative pseudocolour flow cytometry plots showing macrophage distribution by Ly6c and MRC1. G, H: Ly6c$^-$ and MRC1$^+$ macrophages as a proportion of total macrophages in the myocardium. Results are mean ± SEM; n = 5 per group. *p < 0.05, **p < 0.01, ***p < 0.001, ****p < 0.0001.

permanent occlusion [20], it is also possible that the neovessels within the infarct in the BMT group might be leaky and might promote some extravasation of blood.

The presence of increased M2 macrophages in the infarct region of BMT mice may be central to the improved post-MI recovery that was observed. The increase in vascularity of the infarct in BMT mice is likely to be related to the pro-angiogenic properties of M2 macrophages, which have been implicated in vascular morphogenesis during development and in post-natal physiological and pathological tissue remodelling [34]. It is possible that the macrophages within the infarcts of BMT mice may mediate more efficient degradation of dead cardiomyocytes than in control infarcts and may have other properties (e.g. antioxidant actions) that secondarily promote the survival of viable cardiomyocytes within the infarct. A more efficient clearing of dead cardiomyocytes would be consistent with the finding of significant iron deposits within the macrophages. The increased vascularity of the infarct could promote cardiomyocyte survival, although this seems less likely in view of the immature morphology of the vessels [21,27,29–31,33,35]. It is also possible that the effects of irradiation on other resident myocardial cells (e.g. fibroblasts, vascular cells or cardiomyocytes) could contribute to the reduced adverse post-MI remodelling in the BMT group.

An increased number of alternatively activated macrophages were present in the hearts of the BMT group not only after infarction but also before MI. Furthermore, we found a higher number of circulating Ly6c$^-$ monocytes in the blood following BMT. In addition, there was evidence of endothelial activation in the myocardial vessels of mice after BMT, as assessed by VCAM-1 staining. These findings suggest that the process of BMT per se may increase both the mobilisation of monocytes into the blood and their recruitment into the myocardium, with a predominance of alternatively activated cells. We found no evidence of intrinsic differences between the BMT and control groups in the in vitro potential to polarise into M1 or M2-type macrophages. Polarisation of macrophages to an M2 phenotype within the myocardium may be promoted by the efferocytosis by macrophages of dead/dying host cells that have been irreparably damaged by irradiation [36,37]. The presence of these cells in the myocardium even before induction of MI, in addition to the higher influx after coronary occlusion, may facilitate the improved recovery after infarction. To our knowledge, these quite substantial effects have not previously been noted and therefore have not been taken into account in studies of inflammatory mechanisms in which BMT was employed as an experimental strategy.

Macrophages express CD91 and CD163 which are specific receptors for haem and haemoglobin complexes [18]. Recently, a new subpopulation of MRC1$^+$ macrophages that express both CD91 and CD163 – termed Mhem cells – was described in human atherosclerotic plaques [38,39]. It was proposed that haem derived from intraplaque haemorrhage or from direct erythrophagocytosis drives this subset of macrophages, which may have atheroprotective antioxidant properties mediated at least in part through the induction of haem oxygenase-1 [40,41]. In this context, it is of interest that haem-containing macrophages were a very prominent feature of the infarcts in BMT mice. It is possible that the internalisation of haem (derived either from myoglobin or from extravasated blood) may drive the polarisation of macrophages into a Mhem-like phenotype. Although possible effects of Mhem macrophages in the heart have not been reported, it is well established that activation of the haem oxygenase-1 pathways is protective in the setting of

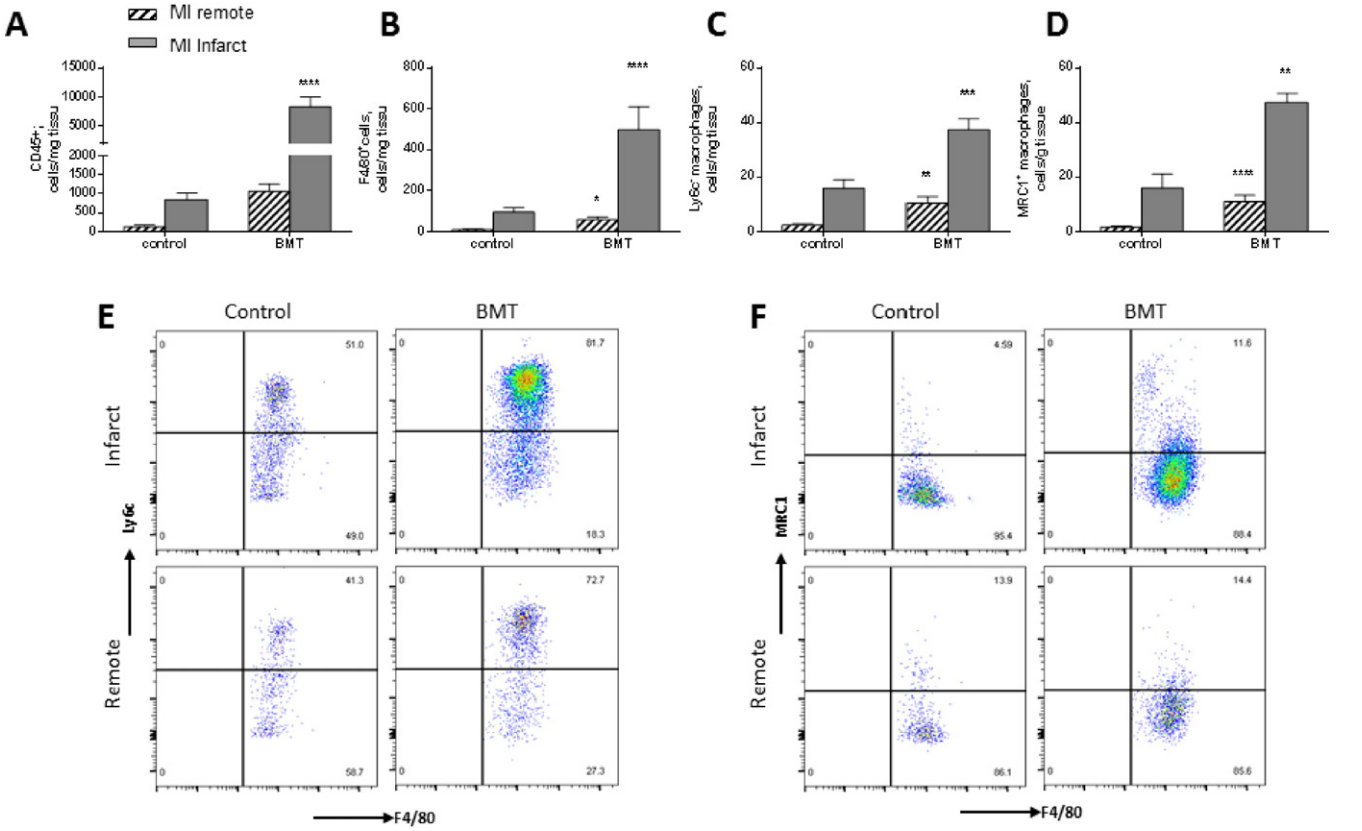

Fig. 6. Flow cytometry analyses of macrophages in the myocardium after acute MI. A–D: Quantification of total leukocytes, macrophages, and macrophage subsets according to Ly6c or MRC1 expression in the infarct and remote regions of control and BMT hearts 4 days after MI. E, F: Representative pseudocolour plots for macrophages based on Ly6c or MRC1 expression. Results are mean ± SEM; n = 5–9 per group. *p < 0.05, **p < 0.01, ***p < 0.001, ****p < 0.0001.

post-MI remodelling [42,43]. Therefore, Mhem-like macrophages could contribute to the protective anti-remodelling effects observed in the present study, a possibility that merits further study.

Based on the findings of the current study, we propose the following scheme to explain the anti-remodelling effects observed after BMT. The process of BMT enhances the mobilisation of monocytes into the blood, their recruitment to the myocardium and/or polarisation to an M2 phenotype, possibly enhanced by the efferocytosis of dying cells. Following coronary occlusion, there is an increased influx of cells into the infarct and the predominance of M2 macrophages facilitates more efficient removal of necrotic cells and tissue and the development of neovessels. Haem derived from cardiomyocyte myoglobin as well as extravasated blood from leaky neovessels may induce the further differentiation of M2 macrophages into a Mhem-like phenotype, which may further enhance tissue repair and cardiomyocyte survival. The overall preservation of ventricular function relates to the presence of a thicker LV wall in the infarct region. However, other effects of radiation on resident cardiac cells could also contribute to the observed reduction in adverse post-MI LV remodelling. The current study highlights the necessity to more carefully interpret the results of experimental studies in which BMT is employed as a tool to distinguish between the effects of BM-derived cells and other cell types.

Disclosures

None of the authors have any disclosures to make.

Acknowledgements

We thank Susanne Heck and PJ Chana for assistance with flow cytometry. These studies were supported by the British Heart Foundation (RG/13/11/30384); a Fondation Leducq Transatlantic Network of Excellence; and the Department of Health via a National Institute for Health Research (NIHR) Biomedical Research Centre award to Guy's & St. Thomas' NHS Foundation Trust in partnership with King's College London and King's College Hospital NHS Foundation Trust.

Appendix A. Supplementary data

Supplementary data to this article can be found online at http://dx.doi.org/10.1016/j.yjmcc.2015.12.007.

References

[1] M.P. de Winther, P. Heeringa, Bone marrow transplantations to study gene function in hematopoietic cells, Methods Mol. Biol. 209 (2003) 281–292.
[2] J.J. Auletta, J.L. Devecchio, J.L. Ferrara, F.P. Heinzel, Distinct phases in recovery of reconstituted innate cellular-mediated immunity after murine syngeneic bone marrow transplantation, Biol. Blood Marrow Transplant. 10 (2004) 834–847.
[3] A.Y. Sheikh, S.A. Lin, F. Cao, Y. Cao, K.E. van der Bogt, P. Chu, et al., Molecular imaging of bone marrow mononuclear cell homing and engraftment in ischemic myocardium, Stem Cells 25 (2007) 2677–2684.
[4] I. Hilgendorf, I. Theurl, L.M. Gerhardt, C.S. Robbins, G.F. Weber, A. Gonen, et al., Innate response activator B cells aggravate atherosclerosis by stimulating T helper-1 adaptive immunity, Circulation 129 (2014) 1677–1687.
[5] P. Blyszczuk, G. Kania, T. Dieterle, R.R. Marty, A. Valaperti, C. Berthonneche, et al., Myeloid differentiation factor-88/interleukin-1 signaling controls cardiac fibrosis and heart failure progression in inflammatory dilated cardiomyopathy, Circ. Res. 105 (2009) 912–920.
[6] M.R. Schroeter, S. Stein, N.M. Heida, M. Leifheit-Nestler, I.F. Cheng, R. Gogiraju, et al., Leptin promotes the mobilization of vascular progenitor cells and neovascularization by NOX2-mediated activation of MMP9, Cardiovasc. Res. 93 (2012) 170–180.
[7] J.S. Burchfield, M. Xie, J.A. Hill, Pathological ventricular remodeling: mechanisms: part 1 of 2, Circulation 128 (2013) 388–400.
[8] M. Nahrendorf, M.J. Pittet, F.K. Swirski, Monocytes: protagonists of infarct inflammation and repair after myocardial infarction, Circulation 121 (2010) 2437–2445.
[9] G. Ren, O. Dewald, N.G. Frangogiannis, Inflammatory mechanisms in myocardial infarction, Curr. Drug Targets Inflamm. Allergy 2 (2003) 242–256.
[10] X. Li, D. Mikhalkova, E. Gao, J. Zhang, V. Myers, C. Zincarelli, et al., Myocardial injury after ischemia-reperfusion in mice deficient in Akt2 is associated with increased

cardiac macrophage density, Am. J. Physiol. Heart Circ. Physiol. 301 (2011) H1932–H1940.
[11] L. Wang, Y.L. Li, C.C. Zhang, W. Cui, X. Wang, Y. Xia, et al., Inhibition of Toll-like receptor 2 reduces cardiac fibrosis by attenuating macrophage-mediated inflammation, Cardiovasc. Res. 101 (2014) 383–392.
[12] P. Krishnamurthy, M. Thal, S. Verma, E. Hoxha, E. Lambers, V. Ramirez, et al., Interleukin-10 deficiency impairs bone marrow-derived endothelial progenitor cell survival and function in ischemic myocardium, Circ. Res. 109 (2011) 1280–1289.
[13] Y. Hu, F. Davison, B. Ludewig, M. Erdel, M. Mayr, M. Url, et al., Smooth muscle cells in transplant atherosclerotic lesions are originated from recipients, but not bone marrow progenitor cells, Circulation 106 (2002) 1834–1839.
[14] A. Protti, X. Dong, A. Sirker, R. Botnar, A.M. Shah, MRI-based prediction of adverse cardiac remodeling after murine myocardial infarction, Am. J. Physiol. Heart Circ. Physiol. 303 (2012) H309–H314.
[15] A. Protti, A. Sirker, A.M. Shah, R. Botnar, Late gadolinium enhancement of acute myocardial infarction in mice at 7T: cine-FLASH versus inversion recovery, J. Magn. Reson. Imaging 32 (2010) 878–886.
[16] J.E. Schneider, F. Wiesmann, C.A. Lygate, S. Neubauer, How to perform an accurate assessment of cardiac function in mice using high-resolution magnetic resonance imaging, J. Cardiovasc. Magn. Reson. 8 (2006) 693–701.
[17] J. Takagawa, Y. Zhang, M.L. Wong, R.E. Sievers, N.K. Kapasi, Y. Wang, et al., Myocardial infarct size measurement in the mouse chronic infarction model: comparison of area- and length-based approaches, J. Appl. Physiol. 102 (2007) 2104–2111.
[18] T.D. Hull, A. Agarwal, J.F. George, The mononuclear phagocyte system in homeostasis and disease: a role for heme oxygenase-1, Antioxid. Redox Signal. 20 (2014) 1770–1788.
[19] M.A. Cavasin, Z. Tao, S. Menon, X.P. Yang, Gender differences in cardiac function during early remodeling after acute myocardial infarction in mice, Life Sci. 75 (2004) 2181–2192.
[20] D.P. O'Regan, R. Ahmed, N. Karunanithy, C. Neuwirth, Y. Tan, G. Durighel, et al., Reperfusion hemorrhage following acute myocardial infarction: assessment with T2* mapping and effect on measuring the area at risk, Radiology 250 (2009) 916–922.
[21] E.J. van den Bos, T. Baks, A.D. Moelker, W. Kerver, R.J. van Geuns, W.J. van der Giessen, et al., Magnetic resonance imaging of haemorrhage within reperfused myocardial infarcts: possible interference with iron oxide-labelled cell tracking? Eur. Heart J. 27 (2006) 1620–1626.
[22] F.Y. McWhorter, T. Wang, P. Nguyen, T. Chung, W.F. Liu, Modulation of macrophage phenotype by cell shape, Proc. Natl. Acad. Sci. 110 (2013) 17253–17258.
[23] K.J. Mylonas, S.J. Jenkins, R.F. Castellan, D. Ruckerl, K. McGregor, A.T. Phythian-Adams, et al., The adult murine heart has a sparse, phagocytically active macrophage population that expands through monocyte recruitment and adopts an 'M2' phenotype in response to Th2 immunologic challenge, Immunobiology 220 (2015) 924–933.
[24] A.P. Beltrami, L. Barlucchi, D. Torella, M. Baker, F. Limana, S. Chimenti, et al., Adult cardiac stem cells are multipotent and support myocardial regeneration, Cell 114 (2003) 763–776.
[25] B.I. Jugdutt, V. Menon, Beneficial effects of therapy on the progression of structural remodeling during healing after reperfused and nonreperfused myocardial infarction: different effects on different parameters, J. Cardiovasc. Pharmacol. Ther. 7 (2002) 95–107.
[26] N.G. Frangogiannis, Regulation of the inflammatory response in cardiac repair, Circ. Res. 110 (2012) 159–173.
[27] M. Nahrendorf, F.K. Swirski, E. Aikawa, L. Stangenberg, T. Wurdinger, J.L. Figueiredo, et al., The healing myocardium sequentially mobilizes two monocyte subsets with divergent and complementary functions, J. Exp. Med. 204 (2007) 3037–3047.
[28] I. Hilgendorf, L.M. Gerhardt, T.C. Tan, C. Winter, T.A. Holderried, B.G. Chousterman, et al., Ly-6Chigh monocytes depend on Nr4a1 to balance both inflammatory and reparative phases in the infarcted myocardium, Circ. Res. 114 (2014) 1611–1622.
[29] J.M. Lambert, E.F. Lopez, M.L. Lindsey, Macrophage roles following myocardial infarction, Int. J. Cardiol. 130 (2008) 147–158.
[30] M.L. Squadrito, F. Pucci, L. Magri, D. Moi, G.D. Gilfillan, A. Ranghetti, et al., miR-511-3p modulates genetic programs of tumor-associated macrophages, Cell Rep. 1 (2012) 141–154.
[31] Y. Takeda, S. Costa, E. Delamarre, C. Roncal, R. Leite de Oliveira, M.L. Squadrito, et al., Macrophage skewing by Phd2 haplodeficiency prevents ischaemia by inducing arteriogenesis, Nature 479 (2011) 122–126.
[32] P. Loke, M.G. Nair, J. Parkinson, D. Guiliano, M. Blaxter, J.E. Allen, IL-4 dependent alternatively-activated macrophages have a distinctive in vivo gene expression phenotype, BMC Immunol. 3 (2002) 7.
[33] A. Mantovani, A. Sica, Macrophages, innate immunity and cancer: balance, tolerance, and diversity, Curr. Opin. Immunol. 22 (2010) 231–237.
[34] S. Nucera, D. Biziato, M. De Palma, The interplay between macrophages and angiogenesis in development, tissue injury and regeneration, Int. J. Dev. Biol. 55 (2011) 495–503.
[35] C. Troidl, H. Mollmann, H. Nef, F. Masseli, S. Voss, S. Szardien, et al., Classically and alternatively activated macrophages contribute to tissue remodelling after myocardial infarction, J. Cell. Mol. Med. 13 (2009) 3485–3496.
[36] P.P. McDonald, V.A. Fadok, D. Bratton, P.M. Henson, Transcriptional and translational regulation of inflammatory mediator production by endogenous TGF-beta in macrophages that have ingested apoptotic cells, J. Immunol. 163 (1999) 6164–6172.
[37] R.E. Voll, M. Herrmann, E.A. Roth, C. Stach, J.R. Kalden, I. Girkontaite, Immunosuppressive effects of apoptotic cells, Nature 390 (1997) 350–351.
[38] J.J. Boyle, Heme and haemoglobin direct macrophage Mhem phenotype and counter foam cell formation in areas of intraplaque haemorrhage, Curr. Opin. Lipidol. 23 (2012) 453–461.
[39] F. De Paoli, B. Staels, G. Chinetti-Gbaguidi, Macrophage phenotypes and their modulation in atherosclerosis, Circ. J.: Off. J. Jpn. Circ. Soc. 78 (2014) 1775–1781.
[40] J.J. Boyle, M. Johns, T. Kampfer, A.T. Nguyen, L. Game, D.J. Schaer, et al., Activating transcription factor 1 directs Mhem atheroprotective macrophages through coordinated iron handling and foam cell protection, Circ. res. 110 (2012) 20–33.
[41] A.V. Finn, M. Nakano, R. Polavarapu, V. Karmali, O. Saeed, X. Zhao, et al., Hemoglobin directs macrophage differentiation and prevents foam cell formation in human atherosclerotic plaques, J. Am. Coll. Cardiol. 59 (2012) 166–177.
[42] M.L. Wu, Y.C. Ho, S.F. Yet, A central role of heme oxygenase-1 in cardiovascular protection, Antioxid. Redox Signal. 15 (2011) 1835–1846.
[43] S.F. Yet, R. Tian, M.D. Layne, Z.Y. Wang, K. Maemura, M. Solovyeva, et al., Cardiac-specific expression of heme oxygenase-1 protects against ischemia and reperfusion injury in transgenic mice, Circ. res. 89 (2001) 168–173.